Interannual variability and climate sensitivity of Net Primary Productivity: a process-based multilayer-canopy vegetation model compared against observed tree-ring width

P. Bodin,[1] P. Alton,[1] and N.Y. Krakauer[2]

Keywords: Land Surface Model, Climate Limitation, Global Carbon Cycle, Dendrochronology

P. Bodin, Geography Department, University of Swansea, Swansea, Wales SA2 8PP, UK. (p.bodin@swansea.ac.uk)

P. Alton, Geography Department, University of Swansea, Swansea, Wales SA2 8PP, UK.

N. Y. Krakauer, Department of Civil Engineering, 193 Steinman Hall, City College of New York, New York, NY 10031, USA.

[1]Geography Department, University of Swansea, UK.

[2]Department of Civil Engineering, City College of New York, USA.

Abstract. For the purpose of modeling future changes in carbon fluxes it is important to correctly simulate the interannual variability (IAV) of global and regional fluxes. Tree-ring data have been used to validate model Net Primary Productivity (NPP) on local or regional scales. Here we present a study, where we used a process-based multilayer-canopy vegetation model forced by a 50-year climate re-analysis dataset. By using an extensive database of tree-ring width (TRW) we quantified how the IAV in model NPP relates to that of tree-ring width. We also mapped regions of climate limitation and quantified regional and global trends in simulated NPP. The magnitude of IAV in TRW and modeled NPP in general agreed but the correlation between TRW and NPP varied greatly between grid cells ($r^2 \leq 0.54$) with the best correlation found in drier regions. Modeled NPP on average showed a weaker correlation with TRW than in studies using site-tuned models. The smaller correlation found in our study can partly be explained by differences in spatial scale but also on the inclusion in our study of regions with long winters, for which modeled NPP seems to correlate less with TRW. Climate limitation of NPP in general agreed with earlier studies and shows precipitation to be the main limiting climatic factor (for 45.5 % of all cells). We estimated a global increase in NPP of 0.32% yr^{-1} for the later half of the 20th century, due primarily to CO_2 fertilization.

1. Introduction

With an increase in atmospheric CO_2 concentration and a concomitant change to climate and its variability [*Prentice et al.*, 2001] many questions emerge on how plants will react to future climate change [*Bonan*, 2008]. Physically based models, which aim to accurately represent the processes involved, can be used for quantifying future fluxes of carbon between plants and the atmosphere.

Due to regional differences in the climatic limitations to plant growth, vegetation at various locations responds differently to changes in climate. By studying these differences in the climatic response of Net Primary Productivity (NPP), regional hotspots for potential sources and sinks of carbon can be identified, that is regions where a change in a climatic driver will have the largest positive or negative effect on NPP.

NPP is affected by changes in climate, most importantly to changes in radiation, temperature and water availability [*Nemani et al.*, 2003; *Hyvönen et al.*, 2007]. The influence of these changes on fluxes of carbon between the atmosphere and the biosphere can be studied using a Land Surface Model (LSM). LSMs are forced with climate data and the interannual variability (IAV) in modeled NPP is influenced by the sensitivity of the model to different climate variables [*Jung et al.*, 2007a]. Several studies have been made on the IAV in modeled NPP [*Dai and Fung*, 1993; *McGuire et al.*, 2001; *Ichii et al.*, 2005; *Ito and Sasai*, 2006; *Jung et al.*, 2007a; *Weber et al.*, 2008; *Piao et al.*, 2009] or NPP from the remotely sensed fraction of absorbed photosynthetically radiation (FAPAR) [*Piao et al.*, 2003; *Mohamed et al.*, 2004]. Globally this IAV is estimated to be $\sim 2\%$ [*Mohamed et al.*, 2004; *Ito and Sasai*, 2006]. Regionally IAV has been found to be much larger (up to 113% [*Dai and Fung*, 1993]), with IAV generally being

larger in drier regions and lower in wetter regions [*Dai and Fung*, 1993; *Knapp and Smith*, 2001; *Fang et al.*, 2001; *Weber et al.*, 2008] although a study by *Mohamed et al.* [2004] found the opposite relationship at a biome scale.

IAV in modeled [*Dai and Fung*, 1993; *Ito and Oikawa*, 2000; *McGuire et al.*, 2000; *Berthelot et al.*, 2002; *Ichii et al.*, 2005; *Jung et al.*, 2007a; *Piao et al.*, 2009] or remotely sensed [*Zhou et al.*, 2003; *Cao et al.*, 2004; *Mohamed et al.*, 2004] NPP in combination with climate data have also been used to study the regional differences in climate sensitivity and to locate the most limiting climate variable. Other similar studies have used predefined climate limitation functions ranging from 0 (no climate limitation) to 1 (full limitation) and observed climate [*Churkina and Running*, 1998; *Nemani et al.*, 2003]. The above studies generally found temperature to be limiting in the north and precipitation in the temperate latitudes. In the tropics NPP is mostly found to be negatively correlated with temperature [*Ito and Oikawa*, 2000; *Berthelot et al.*, 2002; *Cao et al.*, 2004; *Ichii et al.*, 2005; *Piao et al.*, 2009] and positively correlated with radiation [*Churkina and Running*, 1998; *Ito and Oikawa*, 2000; *Berthelot et al.*, 2002; *Nemani et al.*, 2003; *Ichii et al.*, 2005].

Similar to NPP, tree-ring growth also displays a strong IAV. This IAV has previously been correlated with climate data in order to be used as proxies for historic climate [e.g. *Briffa et al.*, 2004]. However, several studies report that the relationship between tree-ring width (TRW) and climate is not straightforward [e.g. *D'Arrigo et al.*, 2008] with some regions showing no sensitivity of TRW to temperature [*Rocha et al.*, 2006] and with a changing relationship between TRW and temperature for some boreal forests over the last 50 years [*Briffa*, 1998]. Stem increment is dependent on the physical processes that determine growth (e.g. photosynthesis and carbon allocation) and stemwood production has been found to be linearly related to gross

primary productivity (GPP) for a wide range of trees and locations [*Litton et al.*, 2007] and with site net ecosystem productivity (NEP) measured from CO_2 eddy covariance [*Rocha et al.*, 2006]. On a local scale, stem growth or NPP simulated with physiological models has been found to correlate reasonably well with TRW ($r^2 = 0.44 - 0.67$) when optimizing the models against TRW data [*Hogg*, 1999; *Misson*, 2004; *Misson et al.*, 2004]. The correlation between TRW and model estimates based on the CASA model forced with a remotely sensed normalized difference vegetation index (NDVI) was even higher ($r^2 = 0.62 - 0.76$) [*Malmström et al.*, 1997]. Using non-optimized models the correlation varies strongly between sites ($r^2 = 0.02 - 0.66$) [*Rathgeber et al.*, 2003; *Berninger et al.*, 2004; *Su et al.*, 2007; *Girardin et al.*, 2008].

Several intercomparison studies of the IAV in simulated global fluxes of carbon have been made [*Friedlingstein et al.*, 2006; *Jung et al.*, 2007b; *Sitch et al.*, 2008; *Weber et al.*, 2008]. However, few studies attempt to validate this simulated IAV. FLUXNET data have frequently been used for model validation [*Ito and Sasai*, 2006; *Friend et al.*, 2007; *Jung et al.*, 2007b] but data are only available for recent years and contain information about NEE and not NPP. For NEE fluxes at a longer time-scale, atmospheric CO_2 can be used for model validation [e.g. *Berthelot et al.*, 2002] but this data typically constrains NEE only over large (continental-scale) regions. Compiled databases of NPP from field measurements exist [e.g. EMDI; *Olson et al.*, 2001] but these contain very little information about its IAV.

The International tree-ring Data Bank (ITRDB) is an extensive collection of publicly available TRW data originally gathered by many researchers over the past decades and representing most parts of the globe (`http://www.ncdc.noaa.gov/paleo/treering.html`). It thus has potential to be used for model validation of IAV in modeled NPP both at long timescales and at a regional spatial scale. The only previous study using multi-site aggregated TRW data for

model validation was based on 21 chronologies of the same species within a 2° grid [*Rathgeber et al.*, 2003]. In this study we use an extensive multi-species TRW database with chronologies from 1955 sites to produce grid-cell aggregates of TRW for validating IAV in NPP from a global model run.

One problem arises when trying to correlate TRW with NPP. Several studies report a time lag between NPP and stem increment [*Fritts*, 1976; *Berninger et al.*, 2004; *Gough et al.*, 2008] or an autocorrelation between years in tree-ring width [*Barford et al.*, 2001; *Monserud and Marshall*, 2001; *Skomarkova et al.*, 2006; *Girardin et al.*, 2008; *Vaganov et al.*, 2009]. This is likely caused by remobilization of carbon and the importance of including this process when modeling TRW is also supported by some modeling studies [*Misson*, 2004; *Misson et al.*, 2004; *Girardin et al.*, 2008]. We therefore expect that TRW might represent a weighted average of previous- and current-year NPP.

In this paper we present a unique modelling study using a multilayer process-based model (JULES) forced with a global climate reanalysis dataset for the years 1948-2000 [*Sheffield et al.*, 2006]. This dataset contains all climate variables needed to drive most LSMs but has never before been used to run a global simulation of carbon fluxes.

Several enhancements have been made to the original LSM to explicitly take account of leaf orientation, diffuse sky radiance and sunfleck penetration [*Alton et al.*, 2007; *Mercado et al.*, 2007; *Alton*, 2008]. These improvements together with the high temporal resolution of the reanalysis climatology (3-hourly) compared to most previous studies [*Cramer et al.*, 2001; *Matthews et al.*, 2005; *Morales et al.*, 2005], ensure that processes such as radiation interception and photosynthesis operating at a sub-daily timescale are realistically simulated.

The objectives of this study are:

1. To quantify the IAV in simulated global NPP and compare it with that of measured TRW.

2. To map regions of climate limitation of NPP using IAV in simulated NPP and in climate variables, and to compare the climate sensitivity of NPP with that of TRW.

3. To quantify both global and regional temporal trends in simulated NPP.

2. Methods

In the following section we describe the LSM used in the study, datasets used, the model run, and the data analysis conducted using the model output and TRW data.

2.1. Model description

JULES is a global LSM based on the Met.Office Surface Exchange Scheme [MOSES *Cox et al.*, 1999]. In this study we used an improved version (JULES-SF) with several important enhancements relating to leaf orientation, diffuse sky radiance, sunfleck penetration [*Alton et al.*, 2007; *Mercado et al.*, 2007; *Alton*, 2008], stomatal conductance [*Ball et al.*, 1987], and plant respiration [*Ryan*, 1991]. JULES uses the standard Penman-Monteith approach [*Monteith*, 1965] for the energy calculation, ensuring a closed energy budget and surface albedo is estimated using the two-stream formulation of *Sellers et al.* [1996]. Vegetation in JULES is separated into 5 Plant Functional Types (PFTs) : broadleaf forest (BL), needleleaf forest (NL), C_3 grassland (C3), C_4 grassland (C4) and shrubland (SH). The model is forced with meteorological variables (downwelling shortwave radiation, downwelling longwave radiation, precipitation, air temperature, windspeed, air humidity and pressure). JULES also requires atmospheric CO_2, biophysical parameters, soil parameters, fractional vegetation cover and LAI. For a more detailed description of JULES-SF see *Cox et al.* [1999] and *Alton and Bodin* [2010].

2.2. Datasets

The Princeton Dataset, a 53 year, 3-hourly meteorology dataset at 1° resolution [*Sheffield et al.*, 2006] was used (available at `http://hydrology.princeton.edu`, accessed 15 Mar 2009) to force the model. This dataset has been constructed by combining several global obseravtion-based datasets and removing known biases in each.

Biophysical parameters were taken from *Alton and Bodin* [2010]. For each PFT the optimal values for the 5 most influential parameters from this study were used and the remaining parameter values were taken from the literature [See Table 1: *Alton and Bodin*, 2010]. Where the optimized value for a parameter differed between PFTs for a parameter which in JULES is taken to have the same value for all PFTs, an area-weighted average of the optimized values for the different PFTs was calculated.

Annual average CO_2 concentrations were taken from measurements at Mauna Loa [*Keeling et al.*, 2009] for the years 1959-2000 and ice core data from Law Dome [*Etheridge et al.*, 1998] for the period 1948-1958. Vegetational fraction cover was calculated using the International Geosphere-Biosphere Project classification [*IGBP*, 1992; *Hansen and Reed*, 2000] simplified to 5 PFTs for use with JULES/MOSES [*Cox et al.*, 1999]. Soil parameter values were taken from the GSWP2 1° dataset [*Dirmeyer et al.*, 1999], which is based on *Wilson and Henderson-Sellers* [1985].

Monthly LAI for each grid cell was based on calculations made using observed relationships between FAPAR and temperature and precipitation [*Los et al.*, 2006] and the CRU reanalysis dataset [*Mitchell and Jones*, 2005].

TRWs were taken from the ITRDB (`http://www.ncdc.noaa.gov/paleo/treering.html`, accessed 15 May, 2009). For each tree, a detrended tree-ring width time

series was created by dividing absolute values by a 15 year centered running mean [cf. *Krakauer and Randerson*, 2003] in order to remove low-frequency variability which might be due to, for example, tree age effects. Data from all available trees at each site were then averaged to produce a detrended tree-ring width site chronology (TRW_d) for in total 1955 sites. Based on the species code in each site record (`http://web.utk.edu/har126grissino/species.htm`) chronologies were separated into broadleaf and needleleaf sites (corresponding to the BL and NL PFTs in JULES). All available site chronologies within a 3° grid cell were averaged and the variance between sites in the same grid cell was used to derive standard errors (SE) for the mean BL or NL TRW_d at each grid cell.

Müller and Lucht [2007] showed that a Dynamical Global Vegetation Model (DGVM) run was relatively insensitive to spatial resolution (up to $10°$). A resolution of 3° was selected for our study to balance between spatial detail and computational speed. The input datasets with 1° resolution were averaged to the 3° grid and the TRW data were aggregated to the same grid. Only grid cells with TRW averages based on at least 5 chronologies spanning at least 10 years were used in the analysis. This resulted in 95 cells with enough TRW_d data, of which 12 were BL.

2.3. Model run

The model was run for 53 years (1948-2000) with a 3-hourly timestep. The first 3 years were used as a spin-up in order to give realistic values for the initial state variables, so only the period 1951-2000 was considered in the analysis.

2.4. Data analysis

For the analysis below, both annual average climate and simulated NPP were detrended using the same method as for the TRW data, that is by using a 15 year running mean average, creating a detrended NPP, SW, T and PPT (NPP_d, SW_d, T_d and PPT_d).

As several studies report a time lag between photosynthesis and stem increment [*Fritts*, 1976; *Gough et al.*, 2008] we used remobilized NPP (NPP_r), to correlate against TRW_d. This was calculated as:

$$NPP_r = c_r NPP_{d,i} + (1 - c_r) NPP_{d,i-1} \quad (1)$$

where c_r is a fitted remobilization parameter ranging from 0 and 1. We also tested two other remobilization models for the correlation: one using previous-autumn simulated NPP and the other, based on *Kagawa et al.* [2006], using a fraction of the current and previous three years' simulated NPP. Neither of these performed better than the simpler model when optimizing the correlation between NPP_r and TRW_d.

As the growing season in the Southern Hemisphere straddles two calendar years, annual modeled NPP in the Southern Hemisphere was calculated as NPP from the second half of the previous year and the first half of the current year.

The NPP_r and TRW_d data were analysed to study: (i) IAV in modeled NPP and TRW, (ii) regions of climatic limitations of NPP, and (iii) trends in modeled NPP.

2.4.1. Interannual variability in modeled NPP and TRW

IAV in NPP_d, calculated as the coefficient of variation (standard deviation normalized to the mean: CV %) between years was compared to the IAV in TRW_d. The correlation between

193 TRW_d and NPP_r was optimized for each grid cell with tree-ring data by using a range of values
194 for c_r between 0 and 1, and the average optimum value for the remobilization constant c_r was
195 calculated using only grid cells with $r^2 \geq 0.2$.

196 **2.4.2. Regions of climatic limitations of NPP**

197 The three detrended climatic variables expected to be most influential (T_d, SW_d and PPT_d)
198 were correlated against modeled NPP_d and the coefficient of correlation (r) was used as a measure
199 of the climate sensitivity of NPP. The influence of each parameter relative to that of all climate
200 variables was calculated by normalising r for each climate-NPP correlation to the sum of r for
201 all climate correlations resulting in a number between 0-1. This was done to quantify the relative
202 importance of each of the three climate variables for NPP at each grid cell. By using r instead
203 of r^2 we include the direction of influence on NPP with 1 on our normalised scale representing
204 $r = 1$ and 0 representing $r = -1$

205 The correlation between climate and TRW_d was calculated using remobilized climate calcu-
206 lated in the same way as NPP_r. The remobilization constant c_r for this calculation was assumed
207 to have the same value as found in the optimization in 2.4.1.

208 **2.4.3. Trends in modeled NPP**

209 For grid cells with significant linear trends ($p \leq 0.05$) in modeled NPP, the annual trend (%)
210 was mapped.

3. Results and Discussion

3.1. Interannual variability in modeled NPP and TRW

211 Annual global simulated NPP averaged 73.4 Gt yr^{-1}. This is above the range of 39.7-70.0 Gt
212 yr^{-1} found in earlier studies using either LSMs or remotely sensed data [*Cramer et al.*, 1999;

Nemani et al., 2003; *Running et al.*, 2004; *Ito and Sasai*, 2006; *Williamson et al.*, 2006; *Huston and Wolverton*, 2009; *Kato et al.*, 2009; *Piao et al.*, 2009; *Zhang et al.*, 2009; *Alton and Bodin*, in preparation]. Many of the early studies however used a constant and relatively low CO_2 levels which could explain some of the difference. Also, the choice of reanalysis meteorology for a model simulation can have a large effect. *Ito and Sasai* [2006] found simulated NPP for 2 models to be 16 and 43% larger if using the NCEP/NCAR dataset [*Kalnay et al.*, 1996] compared to using the ERA40 reanalysis [*Uppala et al.*, 2005] (with one of the latter simulations generating the low end of the range given above).

IAV in simulated global detrended NPP (using a 15-year running mean) was 1.3% with a maximum anomaly of 2.5% for the simulation period. *Ito and Oikawa* [2000] found a maximum anomaly for 1970-1997 of 2.0%. For the period 1982-2001 *Ito and Sasai* [2006] found global IAV to be between 1.4-2.8% in modeled non-detrended NPP and for the period 1987-1997 *Mohamed et al.* [2004] found IAV to be 2.4%. We found global IAV in non-detrended NPP to be 2.7% for the period 1980-2000 .

IAV at single grid cells was larger with an average of 17.9%, and a range of 1-470%. Most cells displayed an IAV of less than 20% (76% of the cells) whereas 8.5% of the cells had an IAV of more than 50%. The cells with high IAV were mainly located in dry regions (Figure 1). This is in line with most previous studies [*Dai and Fung*, 1993; *Fang et al.*, 2001; *Knapp and Smith*, 2001; *Weber et al.*, 2008].

Grid cells where the standard error in TRW_d was larger than the IAV in NPP_d were filtered out leaving 77 cells for the IAV comparison.

For the 77 cells used in this analysis, average IAV was similar for NPP_d and TRW_d with an average of 12.7% in TRW_d and 12.9% in NPP_d. The IAV for NPP_d was also correlated to the IAV in TRW_d (r^2=0.46) (Figure 2) with the correlation being close to 1:1.

Out of the 77 grids, only 19 cells (25%) displayed a correlation between NPP_r and TRW_d with $r^2 \geq 0.2$ when using the optimum value of c_r for that cell (Table 1). Based on these cells, the average optimal value for c_r was 0.27 (+/-0.30). In the literature, the ratio of current year to previous year assimilates found in tree-rings is reported to have a value of 0.54-0.66 [*Kagawa et al.*, 2006; *von Felten et al.*, 2007; *Gough et al.*, 2009] thus indicating that carbon remobilization cannot explain all of the timelag found in the relationship in NPP and TRW. Since only 7 grid cells out of the 77 were BL, the analysis was not carried out separately for BL and NL cells.

The average correlation between NPP_r and TRW_d for all cells was r^2=0.13 with a maximum of 0.54. For a process-based model (MAIDEN), taking into account the remobilization of carbon and optimized for the correlation between modeled and measured TRW at single sites, the maximum correlation was r^2=0.67 [*Misson*, 2004; *Misson et al.*, 2004]. It is not reasonable to expect our model to correlate better, given the relative coarseness of our model grid and the fact that our model correlation with TRW data was optimized using only one parameter (c_r) whereas the MAIDEN model was parameterized with 12 parameters. An unoptimized model yielded a correlation between modeled and simulated NPP (based on tree-ring width and density) of r^2=0.02-0.66 and yielded 0.43 when aggregated regionally [*Rathgeber et al.*, 2003]. The sites used in their study (n=21) were all located in Provence (France) within a 2° range and at similar altitude (160-650 m). In our study only 3 grid cells showed better correlation between TRW_d and NPP_r than the averaged correlation in the study by *Rathgeber et al.* [2003].

The grid cells in our study displaying some correlation between NPP_r and TRW_d ($r^2 \geq 0.2$) are mainly located in the southwestern USA, southern Europe and Turkey whereas cells in north-eastern USA, Canada, Alaska, British Isles and Fennoscandia generally give poor correlations. Several factors could cause these regional differences in the agreement between modeled NPP_r and TRW_d as we now discuss.

Wood mass increment is not fully proportional to TRW since this also depends on the density of the wood which differs between early- and latewood [*Fritts*, 1976]. Early- and latewood densities also vary with location [*Schweingruber*, 1988; *Savva et al.*, 2002] and species [*Schweingruber*, 1988]. There may also be differences between species in the remobilization of carbon [*Barbaroux and Bréda*, 2002]. The aggregation of TRW data, potentially averaged over several species within the same grid cell, may therefore affect the fit between modeled NPP_r and TRW_d. In our study, we only took into account the difference between BL and NL species when creating the grid averages of chronologies.

The spatial heterogeneity within each grid will also have an effect and theoretically NPP should correlate better where climate varies little within the grid and where the trees cored are all representative of the grid (e.g. at a typical altitude). Further, many of the TRW sites are selected based on their location in extreme climate (e.g. high altitudes or latitudes) and for grid cells where TRW measurements have been made at high altitudes TRW data may not be representative for the entire cell. For grid cells in our study elevation variability was calculated as the CV in elevation for all 1° grid cells within each 3° cell (using elevation data from http://islscp2.sesda.com). None of the cells with CV>115% (n=3) showed any correlation between NPP_r and TRW_d thus indicating that a large variabilty in elevation could contribute to the difference between observed NPP and observed TRW.

Further, it has been suggested that tree growth is not closely related to primary productivity, especially in colder regions where tree growth instead is said to be constrained by the temperature limitation of tissue formation [*Körner*, 2003]. Only 6.5% of the grid cells where the temperature was below freezing for more than 1/3 of the year (n=31) showed a correlation of $r^2 \geq 0.2$ whereas 37% of the remaining cells showed such correlation. A study from northern Scandinavia showed that TRW was correlated to previous year NPP and current year nitrogen mineralization calculated from summer mean monthly temperatures [*Berninger et al.*, 2004] thus indicating a temperature effect on TRW not directly connected to NPP.

Previous studies finding relatively good correlation between modeled NPP and TRW have mostly been made on trees located in temperate regions [*Grote and Erhard*, 1999; *Rathgeber et al.*, 2003; *Misson*, 2004] or on the border of the boreal zone [*Hogg*, 1999], that is in regions where temperature limitation of growth is less severe. These studies have also used local climate data from meteorological stations and a single species for each site. Aggregated relationships between TRW and NPP have been based on a single species and using sites at similar altitudes [*Rathgeber et al.*, 2003]. In studies made in colder regions [*Berninger et al.*, 2004; *Su et al.*, 2007; *Girardin et al.*, 2008] the best correlation between modeled and measured TRW was r^2=0.46 (using an empirical model). The factors discussed above could thus partly explain the better correlation found in earlier studies. Excluding grid cells with many freezing days and high variability in altitude from our results gave a slightly improved average correlation between TRW and NPP with r^2=0.16. The good correlation previously found between estimates of NPP using NDVI data and TRW in a boreal forest [*Malmström et al.*, 1997] suggests that the regional poor correlation found in our study is not due to an inherent lack of correlation between NPP and TRW in these regions. Instead it points at limits in the current model's ability to simulate

NPP variability in cold regions possibly associated with the lack of a dynamic nitrogen cycle in the model, or with unrealistic values for reconstructed LAI in those regions.

3.2. Regions of climatic limitations of NPP

Climate sensitivity measured as the correlation between NPP_d and detrended climate variables was analysed and mapped globally (Figure 3). These maps show that low T is limiting in all polar and most temperate regions. Negative correlations with T occur in most parts of the southern hemisphere and these regions also display a positive correlation against PPT. Regions with negative correlation with PPT also show positive correlations with SW radiation and/or T. Regions that are limited by SW radiation are located in the boreal or the tropical zones.

Figure 4 shows the combined effect of different limitations. It becomes clear that water is the main limiting factor (45.5% of the grid cells). NPP was limited by low temperatures for 20.1% of the grid cells (mainly located in the boreal and temperate zones of the northern hemisphere) and by high temperatures for 5.7% of the grid cells (located in the Amazon and regionally in Africa and South East Asia). Only 2.0% of the grid cells spread out globally were limited by SW radiation. The remaining grid cells showed a weak climate limitation ($r^2 \leq 0.2$) (24.3%) or negative correlation with PPT or SW (2.4%). The results in general agree with previous studies [*Dai and Fung*, 1993; *Churkina and Running*, 1998; *Ito and Oikawa*, 2000; *Berthelot et al.*, 2002; *Nemani et al.*, 2003; *Zhou et al.*, 2003; *Cao et al.*, 2004; *Ichii et al.*, 2005; *Jung et al.*, 2007a; *Piao et al.*, 2009]. In particular our model results agree well with a recent study using the ORCHIDEE model [*Piao et al.*, 2009]. Some minor differences exist compared to their study: for example, they find NPP to be limited by T in southwest Australia whereas we find NPP to be limited by PPT.

Compared to *Nemani et al.* [2003] our study gives much smaller regions where NPP is limited by SW. NPP for these regions is instead limited by low PPT or high T in the south and low T in the north. This may be due to the fact that *Nemani et al.* [2003] use cloudiness and not radiation for their SW limitation while our layered-canopy model allows RUE to increase with increased cloudiness in regions with high incoming radiation [*Alton et al.*, 2007; *Mercado et al.*, 2007; *Alton*, 2008].

For the 77 grid cells with TRW data, modeled NPP_d was most sensitive to low PPT_d for 31 grid cells and T_d for 16 grid cells (Table 1). 24 grid cells showed weak climate response ($r^2 < 0.2$) and 6 grid cells negative correlation between NPP_d and SW_d or PPT_d.

Using a uniform value of 0.3 for c_r TRW_d correlated better with NPP_r than with any single detrended climate variable for 16 grid cells whereas TRW_d correlated better with any detrended climate variable for 15 cells (excluding correlations with r^2<0.2 for both cases). This showed that TRW_d correlates at least as well with NPP_r as with detrended climate.

For dry regions (cells with modeled NPP_d most sensitive to a low PPT_d) (n=31) 4 cells showed a substantial positve correlation between TRW_d and PPT_r ($r^2 \geq 0.2$) (Table 1). 14 of the cells showed a stronger positive correlation with detrended summer monthly (Jun, Jul or Aug) simulated soil moisture content (SMC_d) than with with PPT_r (although only one with $r^2 \geq 0.2$) indicating a possible effect of summer drought on TRW. For three of the cells in dry regions, TRW_d instead correlated better with T_r. The dry regions were also where TRW_d and NPP_r best agreed. 35 % of these cells showed a correlation of $r^2 \geq 0.2$ between TRW_d and NPP_r while for the remaining sites this figure was 17 %.

On average 50% of the variabilty in simulated NPP_d could be explained by the IAV in climate (PPT_d: 26% , T_d: 16%, SW_d: 11%) whereas 18% of the IAV in TRW_d could be explained by current and previous year's climate (PPT_r: 6%, T_r: 7%, SW_r: 5%).

In regions of T limitation (e.g. high latitudes and altitudes), TRW has been shown to be correlated with summer temperatures [*Vaganov et al.*, 1999; *Briffa et al.*, 2002; *Frank and Esper*, 2005; *Büntgen et al.*, 2007; *Grudd*, 2008; *Tuovinen et al.*, 2009] and inversely with winter PPT [*Vaganov et al.*, 1999]. One reason for this is that snow inhibits nitrogen mineralization while a high post-snowmelt temperature increases mineralization [*Vaganov et al.*, 1999; *Jarvis and Linder*, 2000]. We therefore tested the correlation between TRW_d and detrended winter PPT and simulated summer soil temperature ($Tsoil_d$). However, only two grid cells displayed a negative correlation between TRW_d and monthly winter PPT or a positive correlation with $Tsoil_d$ thus indicating that the lack of correlation in cold regions cannot solely be explained by the "missing process" of nitrogen mineralization in JULES.

3.3. Trends in modeled NPP

Global simulated NPP increased with 0.24 Gt yr^{-2} (0.32% yr^{-1}) for the simulation period, using reconstructed LAI (Figure 5). One recent study [*Ito and Sasai*, 2006] found an annual increase for the time period 1982-2001 to be in the range 0.08-0.21 Gt yr^{-2} (0.14-0.39 % yr^{-1}) and for a similar time period *Nemani et al.* [2003] and *Piao et al.* [2009] found the increase in global NPP to be 0.34% yr^{-1} and 0.40% yr^{-1} respectively. For the period 1980-2000 we found an increase of 0.31 Gt yr^{-1} (0.40%), which is the same as the estimate by *Piao et al.* [2009]. Most of the annual increase can be explained by an increase in atmospheric CO_2. A simulation using constant CO_2 only gave an increase in global NPP of 0.03 Gt yr^{-2} (Figure 5). Using a constant phenology (calculated using average monthly values of FAPAR for 1991-2000) did not

affect the global trend in NPP. This is in line with previous studies indicating that IAV in climate is more important for the IAV in NPP than IAV in LAI [*Jung et al.*, 2007a] although [*Malmström et al.*, 1997] suggest NDVI to be very important when simulating NPP using the CASA model.

Recent regional positive trends in simulated NPP (1980-2000) (Figure 6) are in general agreement with *Nemani et al.* [2003] and in good agreement with *Piao et al.* [2003]. The most noticeable differences between our study and *Piao et al.* [2009] can be found in eastern Europe and northern India where we find positive trends in NPP whereas they find negative trends, and regions in northern Canada where we find a large region with a strong positive trend in NPP.

Differences between the studies can be explained by differences in the climate sensitivity of the models used and by the selection of climate data. The JULES-SF model and ORCHIDEE models are similar in their representation of photosynthesis, autotrophic respiration and stomatal conductance but differ slightly regarding radiative transfer, evapotranspiration, water balance and number of PFTs [*Krinner et al.*, 2005; *Alton and North*, 2007; *Vetter et al.*, 2008].

For the NCEP dataset which was used by *Nemani et al.* [2003], a large positive bias exists for SW radiation with a spurious upward trend compared to ground measurements [*Sheffield et al.*, 2006]. These differences as well as biases in T and PPT have been corrected in the Princeton dataset [*Sheffield et al.*, 2006] and the removal of spurious trends and biases could thus explain part of the lack of agreement between our study and *Nemani et al.* [2003]. For example, in northern Canada, which is temperature limited, a temperature increase is found in the Princeton dataset whereas the trend is found to be negative in the NCEP dataset [*Nemani et al.*, 2003].

The difference in NPP trends between our study and *Nemani et al.* [2003] found in the Amazon, Africa and Indochina can partly be explained by SW trends (positive or negative) found in the NCEP dataset [*Nemani et al.*, 2003] not occurring in the Princeton dataset. Also, diffuse radiation

has a higher RUE than direct radiation [*Roderick et al.*, 2001; *Alton and North*, 2007; *Mercado et al.*, 2009] which the PEM model in the *Nemani et al.* [2003] does not take into account. SW brightening will thus have a larger positive effect on NPP in the PEM model than in JULES.

As well as validating IAV, tree-ring width data could potentially also be used for the validation of trends in NPP, but as tree-ring growth varies with age, chronologies need to be detrended using for example a low-pass filter or a smoothing function [*Schweingruber*, 1988]. This needs to be done individually to each chronology and with in total 1955 chronologies this was beyond the scope of this study.

3.4. Caveats and limitations

In this study we used a LSM forced with reconstructed LAI assuming no changes to land use or species composition for the simulation period. The TRW data we used for model validation are a proxy for NPP of standing trees, which should not be affected by plant succession or land use change. Including these processes into the model by using a DGVM also introduces further uncertainties to the model [*Moorcroft*, 2006; *Purves and Pacala*, 2008]. For example, inter-species competition in these models follow rules with weak empirical support [*Cramer et al.*, 2001] and simulated fluxes and ecosystem responses can differ greatly between these models [*Moorcroft*, 2006; *Purves and Pacala*, 2008; *Sitch et al.*, 2008].

Other factors that can affect plant growth on a regional scale and not explicitly represented in JULES include atmospheric pollution such as acidification which can lead to nutrient leaching as well as direct toxic effects on leaves [*Bormann and Likens*, 1979] and tropospheric ozone which can reduce photosynthesis, growth, and other plant functions [*Felzer et al.*, 2007]. Sites used in dendrochronological studies are however generally selected to minimize the noise in the data, that is located where non-climatic factors are minimal [*Fritts*, 1976].

In addition to its direct effect on photosynthesis, increased temperature can also affect NPP through increased nutrient mineralization [*Vaganov et al.*, 1999; *Jarvis and Linder*, 2000] and an increase in the length of the growing season [*Sherry et al.*, 2007; *Slaney et al.*, 2007; *Hall et al.*, in preparation]. Fluxes of nitrogen have previously not been included in LSMs but recent studies indicate the importance of including the dynamics of nitrogen [*Wang and Houlton*, 2009; *Zaehle et al.*, 2010].

To improve the useability of TRW data for model validation, LSMs could incorporate: (i) a carbon allocation scheme which varies over the season with a high use of mobile carbon in spring, a direct use of NPP during summer and a storage of assimilated carbon during autumn [*Gough et al.*, 2009]; (ii) a differentiation into early- and latewood with different wood densities [*Rathgeber et al.*, 2003]; (iii) a lower temperature limit for wood formation [*Körner*, 2003]; and (iv) coupled nitrogen/carbon dynamics [*Wang and Houlton*, 2009; *Zaehle et al.*, 2010].

The MAIDEN model [*Misson et al.*, 2004] includes some of these processes and simulates the seasonal differences in carbon allocation. However, this model lacks somewhat in generality to be useful for simulating NPP at a global scale and has yet to include several important recent findings (as discussed above) relating to processes affecting TRW.

The sites in the ITRDB are generally selected for their usefulness in climate reconstruction and are thus mainly located in regions where a single climate variable is limiting to growth. Using TRW data from locations that are more representative for each grid cell [*Malmström et al.*, 1997] would likely improve the correlation between simulated NPP and TRW.

4. Conclusions

Several modeling studies of global primary productivity using re-analysis climate data exist, but few attempts have been made to validate simulation results on a longer time-scale. Our study, using the JULES model, generates absolute values and trends in NPP that are in general agreement with recent studies using a similar approach [e.g. *Piao et al.*, 2009]. Simulated IAV and climate sensitivity of NPP also agrees with previous studies. Using TRW data aggregated to the grid scale we introduce a unique attempt to validate IAV in modeled NPP with that of TRW. The validation shows some agreement in IAV but also points to limitations.

The magnitude of IAV of regional (3°) NPP agrees with that of TRW. However, underlying causes of variation differ. 50% of modeled IAV in NPP can be explained by current-year climate whereas 18% of the IAV in TRW could be explained by current- and previous-year climate. TRW in general correlates as good with simulated NPP as with any climate variable indicating that simulated NPP on average is a better predictor for TRW than any individual climate variable.

JULES performs somewhat poorer than site-tuned models constrained in order to predict specifically TRW ($r^2 \leq 0.54$ compared to 0.44-0.67). This is not surprising given the difference in the purpose of the models (simulating global fluxes of carbon as opposed to local forest growth) and the difference in spatial scale. Previous studies have used locally observed climate, single species chronologies and aggregated TRW data has been based on chronologies of the same species, at similar elevation and within a relatively small region [*Rathgeber et al.*, 2003].

In general TRW showed weaker correlation with NPP in colder regions and for grid cells with large variability in elevation and better in regions with water limitation. Several plausible reasons exist for the regional differences in correlation found in our study.

Suggestions for future model improvement to better use TRW data for model validation include a carbon allocation scheme that includes remobilization of carbon, the differentiation into late- and earlywood, and a lower temperature limit to wood formation. A dynamic nitrogen model could improve the simulation of NPP in colder climates. Much of the details regarding the factors affecting tree-ring formation are still uncertain and more research is needed to better understand these processes.

The fraction of land surface where NPP is most limited by preceipitation, temperature and shortwave radiation is 45.5, 25.8 and 2.0 % respectively. Regional patterns of climate limitation in general agreed with earlier studies [*Nemani et al.*, 2003; *Piao et al.*, 2009] but with a smaller region of SW limitation than in *Nemani et al.* [2003], due to a more complete treatment of light saturation and penetration through multiple canopy layers in the current study.

We estimate a global increase in NPP of 0.32% yr^{-1} over the period 1951-2000. This is in approximate agreement with previous studies. Most of this increase can be attributed to CO_2 fertilization rather than climate change.

Acknowledgments. We thank Andreas Heckel and Sietse Los at Swansea University for assistance in data management, programming and for providing FAPAR data. We also thank Arif Ali at OCF and the Mike Barnsley Centre for Climate Research for helping make JULES run on the Blue Ice supercomputer. PB and PA were supported by the Natural Environment Research Council (NERC) under grant NE/F00205X/1. NYK was supported by the National Oceanic and Atmospheric Administration (NOAA) under Grant Number NA06OAR4810162.

References

Alton, P. (2008), Reduced carbon sequestration in terrestrial ecosystems under overcast skies compared to clear skies, *Agric. For. Meteorol.*, *148*(10), 1641–1653.

Alton, P., and P. Bodin (2010), A comparative study of a multilayer and a productivity (light-use) efficiency land-surface model over different temporal scales, *Agric. For. Meteorol.*, *150*(2), 182–195.

Alton, P., and P. Bodin (in preparation), Model estimates of the continental and oceanic contributions to biospheric carbon and water fluxes using modis satellite data.

Alton, P., and P. North (2007), Interpreting shallow, vertical nitrogen profiles in tree crowns: A three-dimensional, radiative-transfer simulation accounting for diffuse sunlight, *Agric. For. Meteorol.*, *145*(1-2), 110–124.

Alton, P., P. North, and S. Los (2007), The impact of diffuse sunlight on canopy light-use efficiency, gross photosynthetic product and net ecosystem exchange in three forest biomes, *Global Change Biol.*, *13*(4), 776–787.

Ball, J., I. Woodrow, and J. Berry (1987), A model predicting stomatal conductance and its contribution to the control of photosynthesis under different environmental conditions, *Prog. Photosynth. Res.*, *4*, 221–224.

Barbaroux, C., and N. Bréda (2002), Contrasting distribution and seasonal dynamics of carbohydrate reserves in stem wood of adult ring-porous sessile oak and diffuse-porous beech trees, *Tree Physiol.*, *22*(17), 1201.

Barford, C., et al. (2001), Factors controlling long-and short-term sequestration of atmospheric CO_2 in a mid-latitude forest, *Science*, *294*(5547), 1688.

Berninger, F., P. Hari, E. Nikinmaa, M. Lindholm, and J. Merilainen (2004), Use of modeled photosynthesis and decomposition to describe tree growth at the northern tree line, *Tree Physiol.*, *24*, 193–204.

Berthelot, M., P. Friedlingstein, P. Ciais, P. Monfray, J. Dufresne, H. Le Treut, and L. Fairhead (2002), Global response of the terrestrial biosphere to CO_2 and climate change using a coupled climate-carbon cycle model, *Global Biogeochem. Cycles*, *16*(4), 1084.

Bonan, G. (2008), Forests and climate change: forcings, feedbacks, and the climate benefits of forests, *Science*, *320*(5882), 1444.

Bormann, F., and G. Likens (1979), Pattern and process in a forested ecosystem. 253 pp, *New York, Heidelberg, Berlin*.

Briffa, K. (1998), Trees tell of past climates: but are they speaking less clearly today?, *Philos. Trans. R. Soc., B*, *353*(1365), 65.

Briffa, K., T. Osborn, F. Schweingruber, P. Jones, S. Shiyatov, and E. Vaganov (2002), Tree-ring width and density data around the Northern Hemisphere: Part 1, local and regional climate signals, *The Holocene*, *12*(6), 737.

Briffa, K., T. Osborn, and F. Schweingruber (2004), Large-scale temperature inferences from tree rings: a review, *Global Planet. Change*, *40*(1-2), 11–26.

Büntgen, U., D. Frank, R. Kaczka, A. Verstege, T. Zwijacz-Kozica, and J. Esper (2007), Growth responses to climate in a multi-species tree-ring network in the Western Carpathian Tatra Mountains, Poland and Slovakia, *Tree Physiol.*, *27*(5), 689.

Cao, M., S. Prince, J. Small, and S. Goetz (2004), Remotely sensed interannual variations and trends in terrestrial net primary productivity 1981–2000, *Ecosystems*, *7*(3), 233–242.

Churkina, G., and S. Running (1998), Contrasting climatic controls on the estimated productivity of global terrestrial biomes, *Ecosystems*, *1*(2), 206–215.

Cox, P., R. Betts, C. Bunton, R. Essery, P. Rowntree, and J. Smith (1999), The impact of new land surface physics on the GCM simulation of climate and climate sensitivity, *Climate Dynamics*, *15*(3), 183–203.

Cramer, W., D. Kicklighter, A. Bondeau, B. Moore, G. Churkina, B. Nemry, A. Ruimy, A. Schloss, et al. (1999), Comparing global models of terrestrial net primary productivity(NPP): overview and key results, *Global Change Biol.*, *5*(s 1), 1–15.

Cramer, W., et al. (2001), Global response of terrestrial ecosystem structure and function to CO_2 and climate change: results from six dynamic global vegetation models, *Global Change Biol.*, *7*(4), 357–373.

Dai, A., and I. Fung (1993), Can climate variability contribute to the "missing" CO_2 sink?, *Global Biogeochem. Cycles*, *7*, 599–610.

D'Arrigo, R., R. Wilson, B. Liepert, and P. Cherubini (2008), On the 'Divergence Problem' in Northern Forests: A review of the tree-ring evidence and possible causes, *Global Planet. Change*, *60*, 289–305.

Dirmeyer, P., A. Dolman, and N. Sato (1999), The Global Soil Wetness Project: A pilot project for global land surface modeling and validation, *Bull. Amer. Meteor. Soc*, *80*, 851–878.

Etheridge, D., L. Steele, R. Langenfelds, R. Francey, J.-M. Barnola, and V. Morgan (1998), Historical co_2 records from the law dome de08, de08-2, and dss ice cores., in *Trends: A Compendium of Data on Global Change*, Oak Ridge National Laboratory, Oak Ridge, Tenn., U.S.A.

Fang, J., S. Piao, Z. Tang, C. Peng, W. Ji, A. Knapp, and M. Smith (2001), Interannual variability in net primary production and precipitation, *Science*, *293*(5536), 1723.

Felzer, B., T. Cronin, J. Reilly, J. Melillo, and X. Wang (2007), Impacts of ozone on trees and crops, *Comptes rendus-Géoscience*, *339*(11-12), 784–798.

Frank, D., and J. Esper (2005), Temperature reconstructions and comparisons with instrumental data from a tree-ring network for the European Alps, *Int. J. Climatol.*, *25*(11), 1437–1454.

Friedlingstein, P., et al. (2006), Climate-Carbon Cycle Feedback Analysis: Results from the C^4MIP Model Intercomparison, *J. Clim.*, *19*(14), 3337–3353.

Friend, A., et al. (2007), FLUXNET and modelling the global carbon cycle, *Global Change Biol.*, *13*(3), 610–633.

Fritts, H. (1976), *Tree rings and climate*, Academic Press London.

Girardin, M., F. Raulier, P. Bernier, and J. Tardif (2008), Response of tree growth to a changing climate in boreal central Canada: A comparison of empirical, process-based, and hybrid modelling approaches, *Ecol. Modell.*, *213*(2), 209–228.

Gough, C., C. Vogel, H. Schmid, H. Su, and P. Curtis (2008), Multi-year convergence of biometric and meteorological estimates of forest carbon storage, *Agric. For. Meteorol.*, *148*(2), 158–170.

Gough, C., C. Flower, C. Vogel, D. Dragoni, and P. Curtis (2009), Whole-ecosystem labile carbon production in a north temperate deciduous forest, *Agric. For. Meteorol.*, *149*(9), 1531–1540.

Grote, R., and M. Erhard (1999), Simulation of tree and stand development under different environmental conditions with a physiologically based model, *For. Ecol. Manage.*, *120*(1-3), 59–76.

Grudd, H. (2008), Torneträsk tree-ring width and density AD 500–2004: a test of climatic sensitivity and a new 1500-year reconstruction of north Fennoscandian summers, *Clim. Dynam.*,

31(7), 843–857.

Hall, M., B. Medlyn, M. Räntfors, G. Abramowitz, O. Franklin, and G. Wallin (in preparation), Effects of co_2 and temperature elevation on shoot carbon assimilation rates in norway spruce.

Hansen, M., and B. Reed (2000), A comparison of the IGBP DISCover and University of Maryland 1 km global land cover products, *Int. J. Remote. Sens.*, *21*(6), 1365–1373.

Hogg, E. (1999), Simulation of interannual responses of trembling aspen stands to climatic variation and insect defoliation in western Canada, *Ecol. Modell.*, *114*(2-3), 175–193.

Huston, M., and S. Wolverton (2009), The global distribution of net primary production: resolving the paradox, *Ecol. Monogr.*, *79*(3), 343–377.

Hyvönen, R., et al. (2007), The likely impact of elevated [CO_2], nitrogen deposition, increased temperature and management on carbon sequestration in temperate and boreal forest ecosystems: a literature review, *New Phytol.*, *173*(3), 463–480.

Ichii, K., H. Hashimoto, R. Nemani, and M. White (2005), Modeling the interannual variability and trends in gross and net primary productivity of tropical forests from 1982 to 1999, *Global Planet. Change*, *48*(4), 274–286.

IGBP (1992), Improved global data for land applications, in *IGBP Global Change Report No. 20*, edited by J. Townshend, International Geosphere Biosphere Programme, Stockholm.

Ito, A., and T. Oikawa (2000), A model analysis of the relationship between climate perturbations and carbon budget anomalies in global terrestrial ecosystems: 1970 to 1997, *Climate Res.*, *15*(3), 161–183.

Ito, A., and T. Sasai (2006), A comparison of simulation results from two terrestrial carbon cycle models using three climate data sets, *Tellus, Ser. B*, *58*(5), 513–522.

582 Jarvis, P., and S. Linder (2000), Constraints to growth of boreal forests, *Nature*, *405*(6789),
583 904–905.
584 Jung, M., et al. (2007a), Uncertainties of modeling gross primary productivity over Europe:
585 A systematic study on the effects of using different drivers and terrestrial biosphere models,
586 *Global Biogeochem. Cycles*, *21*(4).
587 Jung, M., G. Le Maire, S. Zaehle, S. Luyssaert, M. Vetter, G. Churkina, P. Ciais, N. Viovy, and
588 M. Reichstein (2007b), Assessing the ability of three land ecosystem models to simulate gross
589 carbon uptake of forests from boreal to Mediterranean climate in Europe, *Biogeosciences*,
590 *4*(4), 647–656.
591 Kagawa, A., A. Sugimoto, and T. Maximov (2006), Seasonal course of translocation, storage
592 and remobilization of 13C pulse-labeled photoassimilate in naturally growing Larix gmelinii
593 saplings, *New Phytol.*, *171*(4), 793–804.
594 Kalnay, E., et al. (1996), The NCEP/NCAR 40-year reanalysis project, *Bull. Am. Meteorol. Soc.*,
595 *77*(3), 437–471.
596 Kato, T., A. Ito, and M. Kawamiya (2009), Multiple temporal scale variability during the twenti-
597 eth century in global carbon dynamics simulated by a coupled climate–terrestrial carbon cycle
598 model, *Clim. Dynam.*, *32*(7), 901–923.
599 Keeling, R., S. Piper, A. Bollenbacher, and J. Walker (2009), Atmospheric co_2 records from
600 sites in the sio air sampling network., in *Trends: A Compendium of Data on Global Change.*,
601 Carbon Dioxide Information Analysis Center, Oak Ridge National Laboratory, Oak Ridge,
602 Tenn., U.S.A., doi:10.3334/CDIAC/atg.035.
603 Knapp, A., and M. Smith (2001), Variation among biomes in temporal dynamics of aboveground
604 primary production, *Science*, *291*(5503), 481.

Körner, C. (2003), Carbon limitation in trees, *J. Ecol.*, *91*(1), 4–17.

Krakauer, N., and J. Randerson (2003), Do volcanic eruptions enhance or diminish net primary production? Evidence from tree rings, *Global Biogeochem. Cycles*, *17*(4), 1118.

Krinner, G., N. Viovy, N. de Noblet-Ducoudré, J. Ogée, J. Polcher, P. Friedlingstein, P. Ciais, S. Sitch, and I. Prentice (2005), A dynamic global vegetation model for studies of the coupled atmosphere-biosphere system, *Global Biogeochem. Cycles*, *19*(1).

Litton, C., J. Raich, and M. Ryan (2007), Carbon allocation in forest ecosystems, *Global Change Biol.*, *13*(10), 2089–2109.

Los, S., G. Weedon, P. North, J. Kaduk, C. Taylor, and P. Cox (2006), An observation-based estimate of the strength of rainfall-vegetation interactions in the Sahel, *Geophys. Res. Lett.*, *33*(16), 16,402.

Malmström, C., M. Thompson, G. Juday, S. Los, J. Randerson, and C. Field (1997), Interannual variation in global-scale net primary production: Testing model estimates, *Global Biogeochem. Cycles*, *11*, 367–392.

Matthews, H., A. Weaver, K. Meissner, N. Gillett, and M. Eby (2005), Terrestrial carbon cycle dynamics under recent and future climate change, *J. Clim.*, *18*(10), 1609–1628.

McGuire, A., J. Clein, J. Melillo, D. Kicklighter, R. Meier, C. Vorosmarty, and M. Serreze (2000), Modelling carbon responses of tundra ecosystems to historical and projected climate: sensitivity of pan-Arctic carbon storage to temporal and spatial variation in climate, *Global Change Biol.*, *6*(Supplement 1), 141–159.

McGuire, A., I. Prentice, N. Ramankutty, T. Reichenau, A. Schloss, H. Tian, L. Williams, and U. Wittenberg (2001), Carbon balance of the terrestrial biosphere in the twentieth century: Analyses of CO_2, climate and land use effects with four process-based ecosystem models,

Global Biogeochem. Cycles, *15*, 183–206.

Mercado, L., C. Huntingford, J. Gash, P. Cox, and V. Jogireddy (2007), Improving the representation of radiation interception and photosynthesis for climate model applications, *Tellus, Ser. B*, *59*(3), 553–565.

Mercado, L., N. Bellouin, S. Sitch, O. Boucher, C. Huntingford, M. Wild, and P. Cox (2009), Impact of changes in diffuse radiation on the global land carbon sink, *Nature*, *458*(7241), 1014–1017.

Misson, L. (2004), MAIDEN: a model for analyzing ecosystem processes in dendroecology, *Can. J. For. Res.*, *34*(4), 874–887.

Misson, L., C. Rathgeber, and J. Guiot (2004), Dendroecological analysis of climatic effects on Quercus petraea and Pinus halepensis radial growth using the process-based MAIDEN model, *Can. J. For. Res.*, *34*(4), 888–898.

Mitchell, T., and P. Jones (2005), An improved method of constructing a database of monthly climate observations and associated high-resolution grids, *Int. J. Climatol.*, *25*(6), 693–712.

Mohamed, M., I. Babiker, Z. Chen, K. Ikeda, K. Ohta, and K. Kato (2004), The role of climate variability in the inter-annual variation of terrestrial net primary production (NPP), *Sci. Total Environ.*, *332*(1-3), 123–137.

Monserud, R., and J. Marshall (2001), Time-series analysis of δ 13C from tree rings. I. Time trends and autocorrelation, *Tree Physiol.*, *21*(15), 1087.

Monteith, J. (1965), Evaporation and environment., in *Symp. Soc. Exp. Biol.*, vol. 19, p. 205.

Moorcroft, P. (2006), How close are we to a predictive science of the biosphere?, *Trends Ecol. Evol.*, *21*(7), 400–407.

Morales, P., et al. (2005), Comparing and evaluating process-based ecosystem model predictions of carbon and water fluxes in major European forest biomes, *Global Change Biol.*, *11*(12), 2211–2233.

Müller, C., and W. Lucht (2007), Robustness of terrestrial carbon and water cycle simulations against variations in spatial resolution, *J. Geophys. Res., [Atmos.]*, *112*, 6105.

Nemani, R., C. Keeling, H. Hashimoto, W. Jolly, S. Piper, C. Tucker, R. Myneni, and S. Running (2003), Climate-driven increases in global terrestrial net primary production from 1982 to 1999, *Science*, *300*(5625), 1560.

Olson, R., J. Scurlock, S. Prince, D. Zheng, and K. Johnson (2001), NPP multi-biome: NPP and driver data for ecosystem model, data intercomparison, *Data set. Available on-line [http://www. daac. ornl. gov] from the Oak Ridge National Laboratory Distributed Active Archive Center, Oak Ridge, Tennessee, USA doi*, *10*.

Piao, S., J. Fang, L. Zhou, Q. Guo, M. Henderson, W. Ji, Y. Li, and S. Tao (2003), Interannual variations of monthly and seasonal normalized difference vegetation index (NDVI) in China from 1982 to 1999, *J. Geophys Res., [Atmos.]*, *108*(D14), 4401.

Piao, S., P. Ciais, P. Friedlingstein, N. de Noblet-Ducoudré, P. Cadule, N. Viovy, and T. Wang (2009), Spatiotemporal patterns of terrestrial carbon cycle during the 20th century, *Global Biogeochem. Cycles*, *23*(4).

Prentice, I., et al. (2001), The Carbon Cycle and Atmospheric Carbon Dioxide, Chapter 3: IPCC Climate Change 2001, Working Group 1, The Scientific Basis.

Purves, D., and S. Pacala (2008), Predictive models of forest dynamics, *Science*, *320*(5882), 1452.

672 Rathgeber, C., A. Nicault, J. Kaplan, and J. Guiot (2003), Using a biogeochemistry model in
673 simulating forests productivity responses to climatic change and [CO_2] increase: example of
674 Pinus halepensis in Provence (south-east France), *Ecol. Modell.*, *166*(3), 239–255.
675 Rocha, A., M. Goulden, A. Dunn, and S. Wofsy (2006), On linking interannual tree ring vari-
676 ability with observations of whole-forest CO_2 flux, *Global Change Biol.*, *12*(8), 1378–1389.
677 Roderick, M., G. Farquhar, S. Berry, and I. Noble (2001), On the direct effect of clouds and
678 atmospheric particles on the productivity and structure of vegetation, *Oecologia*, *129*(1), 21–
679 30.
680 Running, S., R. Nemani, F. Heinsch, M. Zhao, M. Reeves, and H. Hashimoto (2004), A con-
681 tinuous satellite-derived measure of global terrestrial primary production, *Bioscience*, *54*(6),
682 547–560.
683 Ryan, M. (1991), Effects of climate change on plant respiration, *Ecol. Appl.*, pp. 157–167.
684 Savva, Y., F. Schweingruber, L. Milyutin, and E. Vaganov (2002), Genetic and environmental
685 signals in tree rings from different provenances of Pinus sylvestris L. planted in the southern
686 taiga, central Siberia, *Trees*, *16*, 313–324.
687 Schweingruber, F. (1988), Tree rings: basics and applications of dendrochronology, *Dordrecht*
688 *(The Netherlands): D. Reidel*.
689 Sellers, P., S. Los, C. Tucker, C. Justice, D. Dazlich, G. Collatz, and D. Randall (1996), A revised
690 land surface parameterization (SiB2) for atmospheric GCMs. Part II: The generation of global
691 fields of terrestrial biophysical parameters from satellite data, *J. Clim.*, *9*(4), 706–737.
692 Sheffield, J., G. Goteti, and E. Wood (2006), Development of a 50-year high-resolution global
693 dataset of meteorological forcings for land surface modeling, *J. Clim.*, *19*(13), 3088–3111.

694 Sherry, R., X. Zhou, S. Gu, J. Arnone, D. Schimel, P. Verburg, L. Wallace, and Y. Luo (2007),
695 Divergence of reproductive phenology under climate warming, *Proc. Natl. Acad. Sci. U. S. A.*,
696 *104*(1), 198.
697 Sitch, S., et al. (2008), Evaluation of the terrestrial carbon cycle, future plant geography and
698 climate-carbon cycle feedbacks using five Dynamic Global Vegetation Models (DGVMs),
699 *Global Change Biol.*, *14*(9), 2015–2039.
700 Skomarkova, M., E. Vaganov, M. Mund, A. Knohl, P. Linke, A. Boerner, and E. Schulze (2006),
701 Inter-annual and seasonal variability of radial growth, wood density and carbon isotope ratios
702 in tree rings of beech (Fagus sylvatica) growing in Germany and Italy, *Trees-Struct. Funct.*,
703 *20*(5), 571–586.
704 Slaney, M., G. Wallin, J. Medhurst, and S. Linder (2007), Impact of elevated carbon dioxide
705 concentration and temperature on bud burst and shoot growth of boreal Norway spruce, *Tree*
706 *Physiol.*, *27*(2), 301.
707 Su, H., W. Sang, Y. Wang, and K. Ma (2007), Simulating Picea schrenkiana forest productiv-
708 ity under climatic changes and atmospheric CO_2 increase in Tianshan Mountains, Xinjiang
709 Autonomous Region, China, *For. Ecol. Manage.*, *246*(2-3), 273–284.
710 Tuovinen, M., D. McCarroll, H. Grudd, R. Jalkanen, and S. Los (2009), Spatial and temporal
711 stability of the climate signal in northern Fennoscandian pine tree-ring width and maximum
712 density, *Boreas*, *38*(1), 1–12.
713 Uppala, S., et al. (2005), The ERA-40 re-analysis, *Q. J. R. Meteorol. Soc.*, *131*(612), 2961–3012.
714 Vaganov, E., M. Hughes, A. Kirdyanov, F. Schweingruber, and P. Silkin (1999), Influence of
715 snowfall and melt timing on tree growth in subarctic Eurasia, *Nature*, *400*(6740), 149–151.

716 Vaganov, E., E. Schulze, M. Skomarkova, A. Knohl, W. Brand, and C. Roscher (2009), Intra-
717 annual variability of anatomical structure and δ 13 C values within tree rings of spruce and
718 pine in alpine, temperate and boreal Europe, *Oecologia*, *161*(4), 729–745.
719 Vetter, M., et al. (2008), Analyzing the causes and spatial pattern of the European 2003 carbon
720 flux anomaly using seven models, *Biogeosciences*, *5*(2), 561–583.
721 von Felten, S., S. Hättenschwiler, M. Saurer, and R. Siegwolf (2007), Carbon allocation in
722 shoots of alpine treeline conifers in a CO 2 enriched environment, *Trees-Struct. Funct.*, *21*(3),
723 283–294.
724 Wang, Y., and B. Houlton (2009), Nitrogen constraints on terrestrial carbon uptake: Implications
725 for the global carbon-climate feedback, *Geophys. Res. Lett.*, *36*(24), L24,403.
726 Weber, U., et al. (2008), The inter-annual variability of Africa's ecosystem productivity: a
727 multi-model analysis, *Biogeosciences Discussions*, *5*, 4035–4069.
728 Williamson, M., T. Lenton, J. Shepherd, and N. Edwards (2006), An efficient numerical terrestrial
729 scheme (ENTS) for Earth system modelling, *Ecol. Modell.*, *198*(3-4), 362–374.
730 Wilson, M., and A. Henderson-Sellers (1985), A global archive of land cover and soils data for
731 use in general circulation climate models, *Int. J. Climatol.*, *5*, 119–143.
732 Zaehle, S., P. Friedlingstein, and A. Friend (2010), Terrestrial nitrogen feedbacks may accelerate
733 future climate change, *Geophys. Res. Lett.*, *37*(1), L01,401.
734 Zhang, Y., M. Xu, H. Chen, and J. Adams (2009), Global pattern of NPP to GPP ratio derived
735 from MODIS data: effects of ecosystem type, geographical location and climate, *Global Ecol.*
736 *Biogeogr.*, *18*(3), 280–290.
737 Zhou, L., R. Kaufmann, Y. Tian, R. Myneni, and C. Tucker (2003), Relation between interannual
738 variations in satellite measures of northern forest greenness and climate between 1982 and

739 1999, *J. Geophys Res.*, *[Atmos.]*, *108*(D1), 4004.

Table 1. Average correlation and number of grid cells (n) with a correlation of $r^2 \geq 0.2$.

	All data (n=77)			Dry regions[a] (n=31)			Cold regions[b] (n=31)		
NPP_r v. TRW_d [c]									
Average correlation (r^2)	0.13			0.15			0.10		
n with $r^2 \geq 0.2$	19			13			2		
NPP_d v. Climate (SW_d, T_d, PPT_d) [d]									
n with $r > 0, r^2 \geq 0.2$	0	16	31	-	-	-	0	8	7
n with $r < 0, r^2 \geq 0.2$	5	0	1	-	-	-	1	0	1
TRW_d v. Climate (SW_r, T_r, PPT_r) [e]									
n with $r > 0, r^2 \geq 0.2$	0	4	5	0	2	4	0	0	0
n with $r < 0, r^2 \geq 0.2$	2	3	4	0	1	0	1	1	3

[a] Grid cells where simulated detrended Net Primary Productivity (NPP_d) was most sensitive to detrended precipitation (PPT_d) (with a positive correlation).

[b] Grid cells with subzero temperature for more than 1/3 of the year.

[c] The correlation between remobilized simulated Net Primary Productivity (NPP_r) and detrended tree-ring width (TRW_d).

[d] The correlation between NPP_d and detrended climate (SW radiation (SW_d), Temperature (T_d), Precipitation (PPT_d)).

[e] The correlation between TRW_d and a fraction of previous and current year's climate (SW_r, T_r, PPT_r).

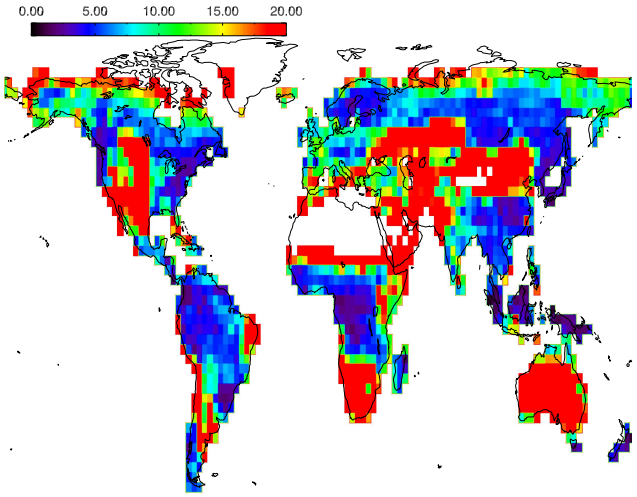

Figure 1. Map of interannual variability (CV%) in detrended simulated annual NPP for the time period 1951-2000.

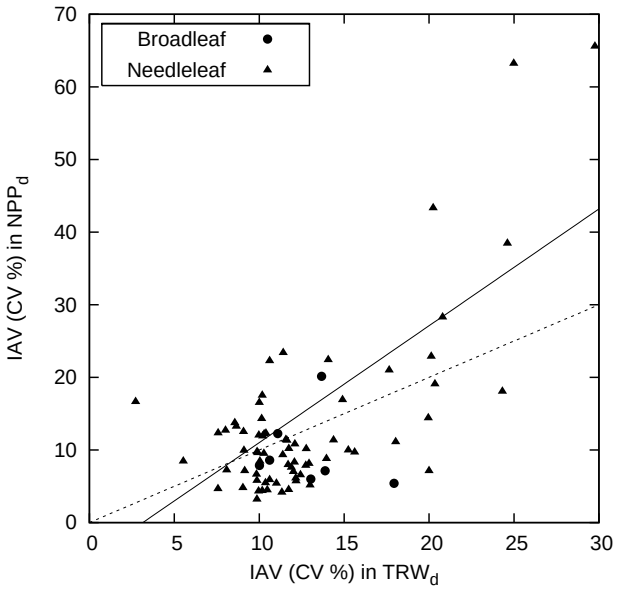

Figure 2. Interannual variability (CV%) in detrended annual values in modeled NPP (NPP_d) and tree-ring width (TRW_d) for both broadleaf (BL) (circles) and needle leaf (NL) grid cells (triangles). The solid regression line represents the best fit using both BL and NL cells and the dashed line represents a 1:1 relationship.

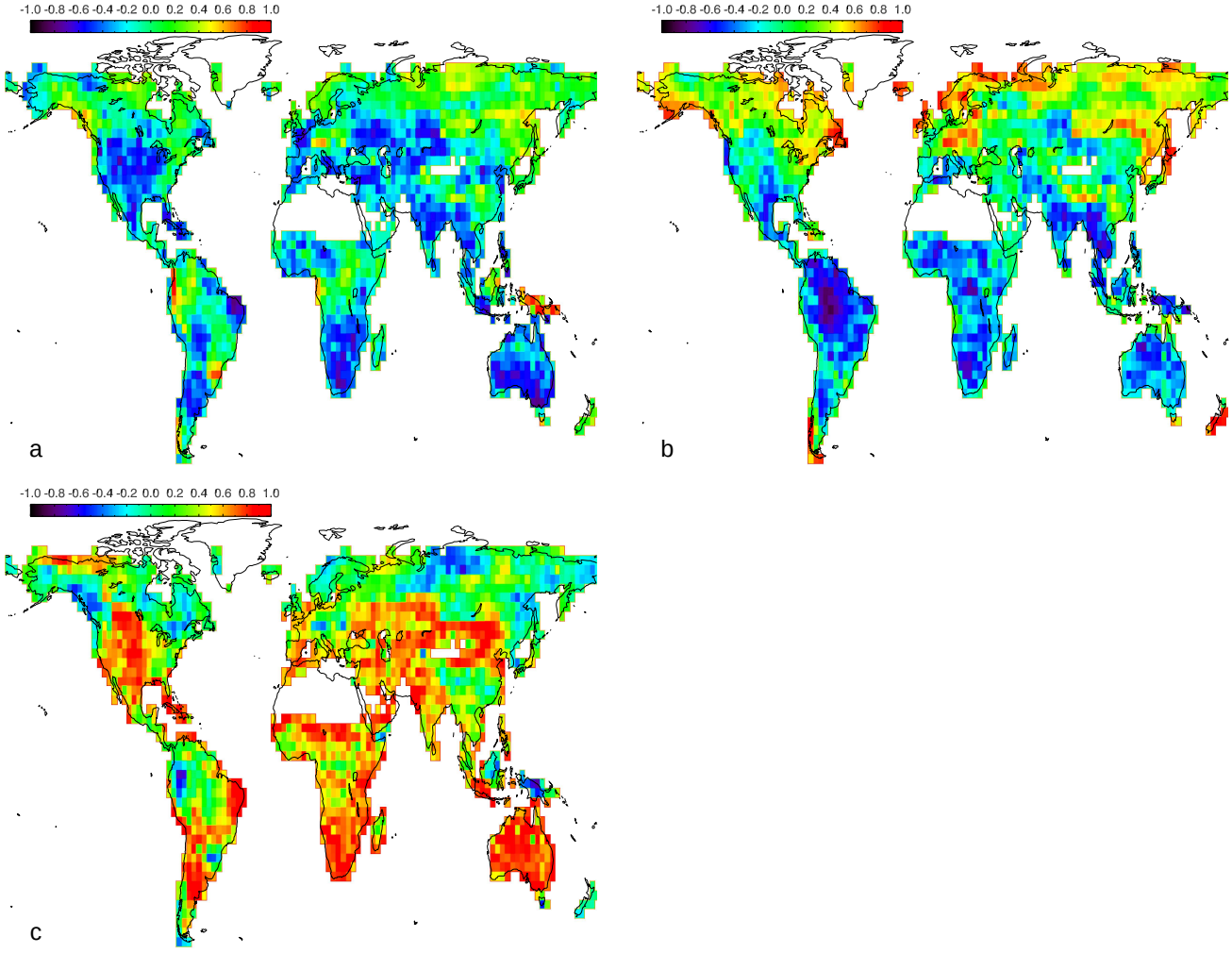

Figure 3. Regional differences in climate sensitivity measured as the the correlation coefficient between modeled NPP and (a) SW radiation, (b) temperature and (c) precipitation.

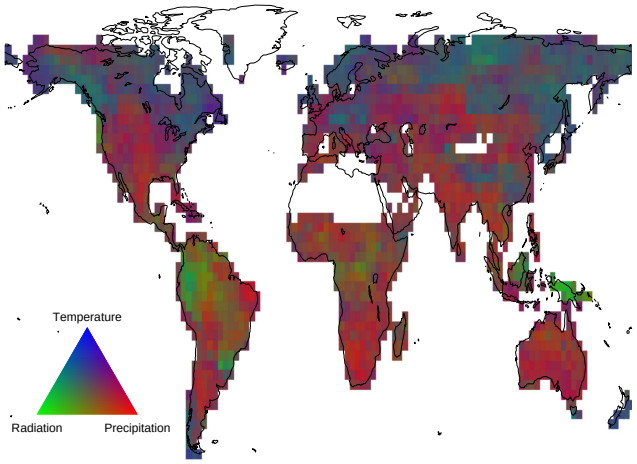

Figure 4. Regional differences in the relative climate sensitivity (for temperature, precipitation and SW radiation) of modeled NPP based on relative correlation strengths between these climate variables and NPP. Red color indicates water limitation, blue temperature limitation, and green limitation of shortwave radiation.

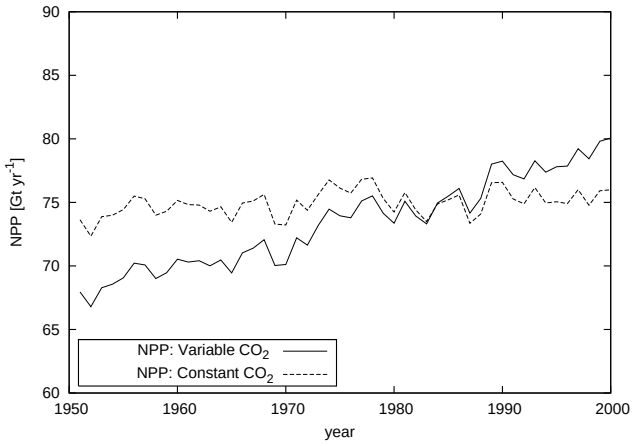

Figure 5. Global simulated annual NPP [Gt yr^{-1}] using variable and constant CO_2.

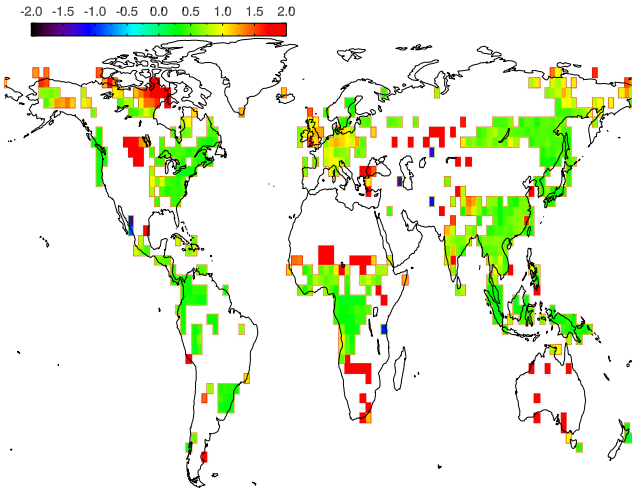

Figure 6. Trends of simulated NPP (% yr^{-1}) for the period 1980-2000. Only grid cells with significant trends ($p \leq 0.05$) are colored.